Title

Climate and soils together regulate photosynthetic carbon isotope discrimination within C3 plants worldwide

Journal

Global Ecology and Biogeography, 27(9)

ISSN

0960-7447

Authors

Cornwell, William K
Wright, Ian J
Turner, Joel
et al.

Publication Date

2018-09-01

DOI

10.1111/geb.12764

Peer reviewed

Received: 21 June 2017 | Revised: 13 May 2018 | Accepted: 22 May 2018

DOI: 10.1111/geb.12764

RESEARCH PAPER

WILEY Global Ecology and Biogeography A Journal of Macroecology

Climate and soils together regulate photosynthetic carbon isotope discrimination within C_3 plants worldwide

William K. Cornwell[1,2] | Ian J. Wright[3] | Joel Turner[2] | Vincent Maire[3,4] | Margaret M. Barbour[5] | Lucas A. Cernusak[6] | Todd Dawson[7] | David Ellsworth[8] | Graham D. Farquhar[9] | Howard Griffiths[10] | Claudia Keitel[5] | Alexander Knohl[11] | Peter B. Reich[8,12] | David G. Williams[13,14] | Radika Bhaskar[15] | Johannes H. C. Cornelissen[1] | Anna Richards[16] | Susanne Schmidt[17] | Fernando Valladares[18] | Christian Körner[19] | Ernst-Detlef Schulze[20] | Nina Buchmann[21] | Louis S. Santiago[22]

[1]Department of Systems Ecology, Institute of Ecological Science, VU Amsterdam, The Netherlands

[2]Ecology and Evolution Research Centre, School of Biological, Earth and Environmental Sciences, University of New South Wales, Kensington, New South Wales, Australia

[3]Department of Biological Sciences, Macquarie University, Sydney, New South Wales, Australia

[4]Département des sciences de l'environnement, Université du Québec à Trois Rivières, Trois Rivières, Québec, Canada

[5]School of Life and Environmental Science, University of Sydney, Sydney, New South Wales, Australia

[6]College of Science and Engineering, James Cook University, Cairns, Queensland, Australia

[7]Department of Integrative Biology, University of California, Berkeley, Berkeley, California

[8]Hawkesbury Institute for the Environment, Western Sydney University, Penrith, New South Wales, Australia

[9]Research School of Biology, The Australian National University, Australian Capital Territory, Acton, Australia

[10]Department of Plant Sciences, University of Cambridge, Cambridge, United Kingdom

[11]Georg-August University of Göttingen, Göttingen, Germany

[12]Department of Forest Resources, University of Minnesota, St Paul, Minnesota

[13]Department of Botany, University of Wyoming, Laramie, Wyoming

[14]Program in Ecology, Department of Ecosystem Science and Management, University of Wyoming, Laramie, Wyoming

[15]Kanbar College, Jefferson University, Philadelphia, Pennsylvania

[16]CSIRO Sustainable Ecosystems, Tropical Ecosystems Research, Winnellie, Northern Territory, Australia

[17]School of Integrative Biology, University of Queensland, St. Lucia, Queensland, Australia

[18]Departamento de Biogeografía y Cambio Global, Museo Nacional de Ciencias Naturales, CSIC & Laboratorio Internacional en Cambio Global CSIC-PUC (LINCGlobal), Madrid, Spain

[19]Institute of Botany, University of Basel, Basel, Switzerland

[20]Max Planck Institute for Biogeochemistry, Jena, Germany

[21]Institute of Agricultural Sciences, ETH Zurich, Zurich, Switzerland

[22]Botany and Plant Sciences Department, University of California, Riverside, Riverside, California

Correspondence
William K. Cornwell, School of Biological, Earth, and Environmental Sciences
The University of New South Wales
UNSW Sydney, NSW 2052 Australia
Email: w.cornwell@unsw.edu.au

Funding Information
ARC-NZ Research Network for Vegetation Function; Netherlands Organization for Scientific Research, Grant/Award Number: 820.01.016.

Abstract

Aim: Within C_3 plants, photosynthesis is a balance between CO_2 supply from the atmosphere via stomata and demand by enzymes within chloroplasts. This process is dynamic and a complex but crucial aspect of photosynthesis. We sought to understand the spatial pattern in CO_2 supply–demand balance on a global scale, via

analysis of stable isotopes of carbon within leaves ($\Delta^{13}C$), which provide an integrative record of CO_2 drawdown during photosynthesis.

Location: Global.

Time period: 1951–2011.

Major taxa studied: Vascular plants.

Methods: We assembled a database of leaf carbon isotope ratios containing 3,979 species–site combinations from across the globe, including 3,645 for C_3 species. We examined a wide array of potential climate and soil drivers of variation in $\Delta^{13}C$.

Results: The strongest drivers of carbon isotope discrimination at the global scale included atmospheric pressure, potential evapotranspiration and soil pH, which explained 44% of the variation in $\Delta^{13}C$. Addition of eight more climate and soil variables (each explaining small but highly significant amounts of variation) increased the explained variation to 60%. On top of this, the largest plant trait effect was leaf nitrogen per area, which explained 11% of $\Delta^{13}C$ variation.

Main conclusions: By considering variation in $\Delta^{13}C$ at a considerably larger scale than previously, we were able to identify and quantify key drivers in CO_2 supply–demand balance previously unacknowledged. Of special note is the key role of soil properties, with greater discrimination on low-pH and high-silt soils. Unlike other plant traits, which show typically wide variation within sets of coexisting species, the global pattern in carbon stable isotope ratios is much more conservative; there is relatively narrow variation in time-integrated CO_2 concentrations at the site of carboxylation among plants in a given soil and climate.

KEYWORDS

carbon isotopes, environmental drivers, global, leaf traits, leaves, soil

1 | INTRODUCTION

Understanding the link between the terrestrial carbon cycle and the water cycle is a fundamental challenge for biogeochemical research. These cycles are inextricably linked by two dynamic supply–demand functions: The first is the supply of water to plants in the soil and the evaporative demand for that water from the atmosphere; the second is the supply of CO_2 from the atmosphere to chloroplasts through the stomata and the enzymatic demand for that CO_2 at the chloroplast. Supply and demand of both water and CO_2 change on the order of seconds, and plants must adjust to constantly changing conditions by closing the stomata to slow water loss, which unavoidably restricts CO_2 supply to the choloroplast. Stomatal aperture is only one of many important factors in plant adaptation to water–carbon dynamics, and this research area continues to be of great importance (Buckley & Mott, 2013; Cernusak et al., 2013; Wolf et al., 2013).

In understanding this complex balancing act, one of the most powerful investigative tools available is the ratio of ^{13}C and ^{12}C, the stable isotopes of carbon (Nier & Gulbransen, 1939). During photosynthesis, respiration and other biogeochemical processes, there are significant changes in the stable isotope ratio, and this creates variation within pools of carbon across the globe. Measurements of carbon isotopic ratios within various C pools have served to develop, constrain and refine models of C cycling at the leaf (Farquhar & Richards, 1984), ecosystem (Beer et al., 2009; Bowling, Tans, & Monson, 2001) and global scales (Kaplan, Prentice, & Buchmann, 2002).

The largest flux of carbon from the atmosphere to the terrestrial biosphere is photosynthesis, with the majority via C_3 photosynthesis (Still, Berry, Collatz, & DeFries, 2003), an enzyme-mediated process that selectively favors $^{12}CO_2$ use relative to $^{13}CO_2$. The analytical description of the degree of isotope discrimination (Farquhar, O'Leary, & Berry, 1982) was a key advance in biogeochemistry; it showed that carbon isotopes can provide a time-integrated record of the partial pressure of CO_2 at the chloroplast (p_c) compared with the partial pressure in the atmosphere (p_a). In brief, if p_c is close to p_a, the enzyme involved in carbon capture can more fully execute its preference for $^{12}CO_2$. Furthermore, the isotopic signature of the resulting plant biomass can be attributed to specific physiological mechanisms, including resistance of CO_2 diffusion from the atmosphere to the site of carboxylation inside the chloroplast. These technical advances allowed a better understanding of individual plant growth and survival, and the response of plants to shifts in

environmental conditions, especially to changes in water availability (Cernusak et al., 2013; Dawson, Mambelli, Plamboeck, Templer, & Tu, 2002; Schulze et al., 1998; Stewart, Turnbull, Schmidt, & Erskine, 1995).

Variation in the isotopic signature of leaves exists at a series of nested scales: Within individuals, among individuals of a species and among species (Farquhar, Ehleringer, & Hubick, 1989). Furthermore, variation among species exists at a given site and across climatic gradients (Brooks, Flanagan, Buchmann, & Ehleringer, 1997). Explanations for the appearance of this variation fall into three broad categories: First, variation in the stomatal aperture in response to biotic and/or abiotic processes (Ehleringer, Field, Lin, & Kuo, 1986; Farquhar & Richards, 1984); second, the biochemical nature of the leaf, especially its carboxylation capacity (Virgona & Farquhar, 1996); and third, the resistance to CO_2 diffusion within the leaf mesophyll (Barbour, Warren, Farquhar, Forrester, & Brown, 2010; Evans, Sharkey, Berry, & Farquhar, 1986). In addition, there are important effects of fractionations within the chemical fractions in the leaf and in both the export of carbon from the leaf to non-photosynthetic tissues (Cernusak et al., 2009) and moving from leaf to ecosystem scales (Brüggemann et al., 2011).

The goal of this work is to examine variation in leaf carbon isotopes at the largest scale, synthesizing hundreds of detailed local studies that have reported carbon isotopes within the leaves of C_3 plants. Although the mechanisms at the leaf level are well characterized, scaling up to the globe is not a trivial task. At the global scale, climatic variation can directly affect isotope discrimination via the mechanisms listed above or indirectly via a shift in the functional traits of the species that are successful at a given place (Wright et al., 2005). Two previous studies have argued that precipitation and elevation (with a possible effect of temperature) are the only significant macroclimatic controls on global leaf carbon stable isotopes (Diefendorf, Mueller, Wing, Koch, & Freeman, 2010; Kohn, 2010). We seek to re-examine this question with a dataset that is more than five times larger than any previous efforts, including a much wider range of both taxa and climates.

To explore how much of the global variation in carbon stable isotopes may be explained by climate and soil variables, we use a model selection approach. This approach generates a data-driven predictive model, mapping multivariate climate to carbon isotope discrimination in C_3 photosynthesis. We also examine the effect of leaf traits. These analyses enable us to generate the most complete, global picture to date of abiotic and biotic effects on carbon isotope discrimination during photosynthesis.

2 | METHODS

We gathered bulk leaf carbon isotopic data from published and unpublished records from vascular plants in natural and semi-natural habitats across the world (see Figure 1 and the Supporting Information). We were especially interested in those studies that simultaneously collected leaf trait and instantaneous gas-exchange data. Although we make no claims to have surveyed the extensive carbon isotope literature exhaustively, the data we collected span the globe, including sites on all seven continents (Figure 1; Supporting Information Figures S1 and S2). These sites represent all major climates types in which C_3 photosynthesis occurs (Supporting Information Figure S1).

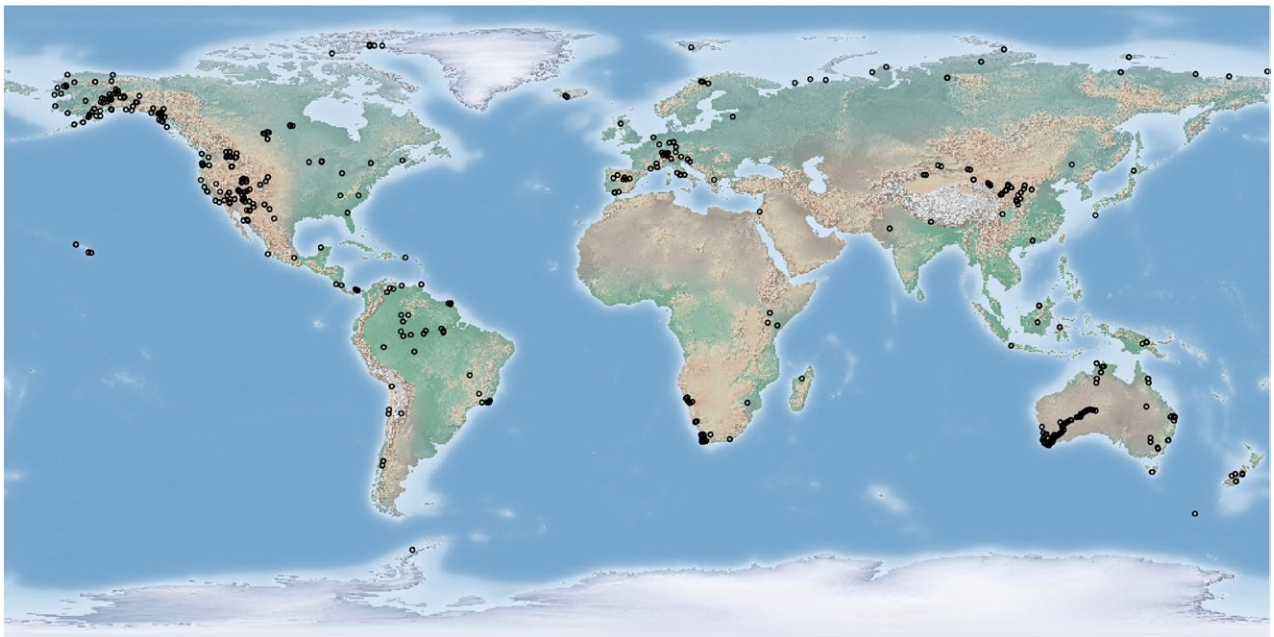

FIGURE 1 Collection locations for the C_3 plants in this analysis. All points are represented by open circles in this figure, but sampling is so dense in some parts of the world that the circles appear filled [Colour figure can be viewed at wileyonlinelibrary.com]

For more details, see the data descriptor (Zenodo https://doi.org/10.5281/zenodo.569501). This analysis considers only the C_3 observations in that database. For most of the analyses presented here, the fundamental "data unit" is a species–site observation. The database includes 3,985 observations from 594 sites on all seven continents. Of those, 3,645 species-by-site combinations were C_3 plants.

2.1 | Climate and soil data

We use the locally measured climatic variables when the original researcher either reported or directly supplied the data. In cases where these data were not available, we used an interpolated climate grid that represents site means for 1961–1990 (New, Lister, Hulme, & Makin, 2002). As would be expected, the interpolated data generally reproduce well the locally measured data, with the exception of areas with extreme topography where orographic rainfall is especially important. In these cases, we made an additional effort to find locally measured climate variables.

Owing to the complexity of plant water relationships, with potential effects of boundary layers, diurnal temperature patterns, freezing events and many other factors, we took an inclusive approach to select potential predictor variables. We sought to use the parameters that could both affect discrimination and be measured or calculated from global interpolated climate grids. A priori, we considered 29 climate and soil variables (see Supporting Information Table S1), including annual means, variables focused on the growing season and those that attempt to capture daily variation. For the growing season, we used the definition of Kikuzawa, Onoda, Wright, and Reich (2013), which estimates the number of months of growing season across the world.

Soil texture, structure and soil ion-exchange capacity of the 0–30 cm layer were extracted from the global, interpolated 30 arc-s Harmonised World Soil Database (FAO, 2012). The soil chemistry from the 0–20 cm layer was extracted from the 5 arc-min ISRIC-WISE dataset (Batjes, 2012). As a result of strong collinearity among many soil texture variables, we chose only two, soil silt percentage and soil clay percentage, to consider in the model selection process. (For a complete list of considered soil variables, see Supporting Information Table S1.) In both datasets, each grid cell includes different soil profiles, with their relative proportion. Insufficient information on soil types was available in the original publications to select the appropriate profile; therefore, we calculated the weighted profile mean of each soil variable within a grid cell.

Soils and climate co-vary as a result of a number of mechanisms, including the development of soils at the global scale (Chadwick, Derry, Vitousek, Huebert, & Hedin, 1999) and recent glaciations (and a reset of soil development) in the far northern hemisphere. Soils at high temperature and high precipitation tend to be more acidic, although there is significant scatter in this relationship, notably some acidic soils from very cold climates (Supporting Information Figure S1). Site estimates for both climate and soil variables were extracted from soil and climate grids using the "extract" function with the "bilinear" option from the "Raster" library (Hijmans, 2014). The only exception to this approach were coastal data points for which there were missing data in surrounding grid cells. In these cases, we used the value from the closest cell only.

2.2 | Plant trait data

In all cases, we made an effort to include leaf trait data measured simultaneously with the carbon isotope data, which were sometimes published along with the isotope values. In some cases, we contacted the original researchers who then contributed previously unpublished data.

There were six plant characteristics that we expected to influence C isotope discrimination. Gas-exchange traits clearly affect the partial pressure of CO_2 at the chloroplast (p_c). However, gas exchange is typically measured instantaneously under non-random (often highly favorable) conditions, so the mapping to carbon isotopes, which are a flux-weighted, integrative measure, is not expected to be exact. We gathered data on maximal rates of photosynthesis (A_{max}) and stomatal conductance (g_{max}), both expressed per unit leaf area. Leaf nitrogen, like carbon isotopes, changes on slower time-scales compared with gas exchange. Leaf nitrogen is known to be correlated with the concentration of the photosynthetic enzyme, ribulose-1,5-bisphosphate carboxylase/oxygenase (RuBisCO), which affects p_c/p_a and carbon isotopes through a drawdown of p_c (Marschner, 2012). We consider nitrogen concentration on both mass and area bases. Specific leaf area (fresh area per dry mass, SLA) may influence both internal drawdown of CO_2 via leaf nitrogen per area and the mesophyll conductance to CO_2 diffusion (Vitousek, Field, & Matson, 1990). Leaf size is a major determinant of boundary layer thickness in low-wind conditions. Thus, under a given radiation stream, larger leaves may experience higher maximal temperatures (which may or may not be beneficial), but also take longer to reach benign temperatures after frost events (Jones, 1992; Jordan & Smith, 1995; Vogel, 1970).

2.3 | Statistical considerations

The covariance of global climate variables is well known (Whittaker, 1975), and the recent emergence of global soil maps has revealed that climate and many aspects of soils also covary strongly (for these specific sites, see Supporting Information Figure S10). As with all analyses of global climate, covariance of predictors is an important consideration, potentially affecting the specific model parameter estimates (Graham, 2003), and thus these should be interpreted with caution. To address this issue, in part, we removed highly covarying predictors a priori (Grueber, Nakagawa, Laws, & Jamieson, 2011). We then used model selection among candidate models using the predictors in Supporting Information Table S1 based on the Bayesian information criterion (BIC; see Kuha, 2004). The final model selection balances explanatory power with parsimony. The step function in base R (Venables & Ripley, 2002) and the model selection and multimodel inference library (Bartoń, 2016) led to identical results. We chose BIC rather than

the more common Akaike information criterion (AIC) because BIC has a stronger penalty for additional parameters (Kuha, 2004), and we felt that a tendency toward model parsimony was appropriate for this question. We began the model selection with potential climate and soil predictor variables (see Supporting Information Table S1) and then iteratively added and subtracted predictors, searching for the model with the lowest BIC. If an individual parameter did not add explanatory power above the penalty for model complexity as defined by the BIC, it was dropped from the model.

If derived from first principles, all of the relationships shown would probably be nonlinear in complex ways (Farquhar et al., 1982). Moreover, the annual (or even daily) climate data would be insufficient to capture all the relevant mechanisms; variables such as annual precipitation are themselves several steps removed from plant water availability. The linear model used here represents a preference for model parsimony in a statistical description of the global variation, not an assertion that these relationships are mechanistically linear.

All analyses were performed in R version 3.2.0 (R Core Team, 2013).

3 | RESULTS

3.1 | Climate- and soil-driven variation

The strongest single climate predictor was annual precipitation (greater discrimination at high precipitation; i.e., higher p_c/p_a during photosynthesis; Figure 2, r^2 = .39), and the strongest single soil predictor was pH (greater discrimination at low pH; Figure 2, r^2 = .35). However, the multivariate analysis pointed to a more complex explanation; adding more climate variables in many cases added explanatory power. A model with three variables, namely atmospheric pressure, potential evapotranspiration (PET) and soil pH, explained 44% of global variation.

Considering all possible variables (see Supporting Information Table S1), the selected model explained 60% of the global variation in discrimination within C_3 plants. The BIC-selected model included 11 separate variables with important explanatory power (Table 1).

Three of the most indispensable predictors, measured by the degree to which a model excluding that variable had diminished performance (ΔBIC within Table 1), were (a) atmospheric pressure, (b) frost frequency, and (c) PET (Table 1). Note that the relationship described in Table 1 is for all C_3 species. The climate association would be even stronger when considering only woody plants (Supporting Information Figure S4) and within woody species, considering only evergreen leaves (Supporting Information Figure S5). Considering only evergreen woody species, the same model selection procedure achieved an $r^2_{adj} = .67$. This is probably because mean annual climate parameters more clearly match the photosynthetic opportunities for evergreen species, whereas winter deciduous, drought deciduous and herbaceous species have different windows for photosynthesis.

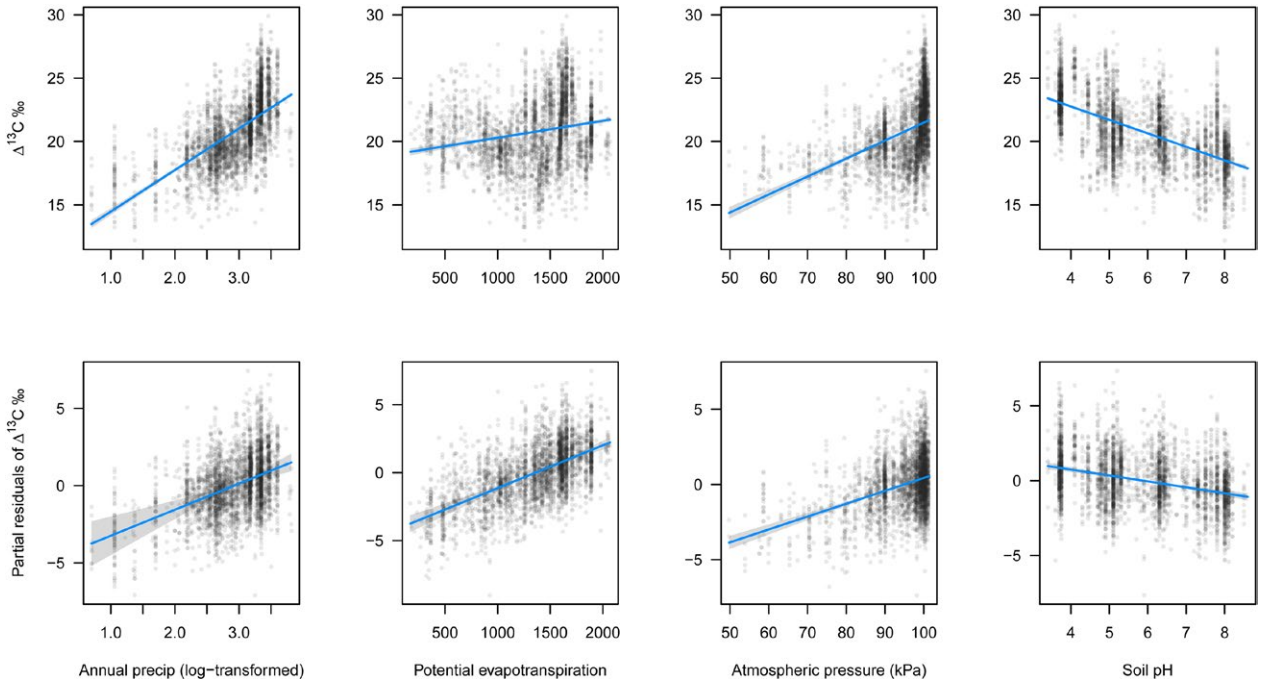

FIGURE 2 The top row shows the raw data for four of the strongest bivariate climate and soil relationships. The parameter estimates for the model in Table 1 are best visualized as partial residual plots, shown in the bottom row of panels, produced using code from Breheny and Burchett (2013). In both rows, the blue line shows the ordinary least squares fit, and the shaded area around it shows one confidence interval (0.95) around the parameter estimates. Note that the model described in Table 1 corresponds to the slopes in the second row, not the first row. See also the full set of partial residual plots in Supporting Information Figure S7 [Colour figure can be viewed at wileyonlinelibrary.com]

TABLE 1 The best model for predicting leaf $\Delta^{13}C$ as selected by Bayesian information criterion

Variable	Coefficient estimate	*SE*	*t*-value	*p*-value	Sensitivity (‰$\Delta^{13}C$)	ΔBIC
Atmospheric pressure	0.085	4.6×10^{-3}	18.7	3.5×10^{-74}	4.39	325.0
Frost frequency	0.016	9.0×10^{-4}	17.6	2.5×10^{-66}	5.12	288.8
Potential evapotranspiration	0.003	2.0×10^{-4}	16.5	5.9×10^{-59}	5.95	254.9
Soil pH	−0.44	0.04	−10.2	3.1×10^{-24}	2.27	95.4
Soil silt	0.037	3.7×10^{-3}	9.9	6.4×10^{-23}	2.12	89.3
Diurnal temperature range	−0.19	0.019	−9.9	7.2×10^{-23}	2.79	89.1
Annual precipitation (log_{10})	−1.1	0.11	9.3	2.0×10^{-20}	3.29	77.9
Seasonality	0.84	0.11	7.6	2.6×10^{-14}	0.84	50.1
Mean wind speed	−0.17	0.03	−5.1	4.5×10^{-07}	1.06	17.4
Number of rain days	0.004	0.001	4.1	4.5×10^{-05}	1.14	8.6
Growing season length	0.05	0.014	3.6	3.2×10^{-04}	0.64	4.9
(Intercept)	7.27	0.74	9.8	1.6×10^{-22}		

Note. As with all analyses of global climate, predictor covariance is a problem, and the slope estimates may be unstable among strongly covarying predictors (Graham, 2003). The model selection approach began with 29 soil and climate variables (see Supporting Information Table S1). The 11 variables listed added significant information to the model over and above the preference for model simplicity inherent in the Bayesian information criterion (BIC). A few data points had to be excluded owing to incomplete coverage of the climate and/or soil layers (e.g., points on Antarctica). The overall $r^2_{adj}=0.60$. *F*-statistic: 419.7 on 11 and 3,533 degrees of freedom. *p*-value: $<10^{-15}$. Sixty-three observations in the full database needed to be removed from the model owing to missing soil data. The coefficient estimate is the equation for the best-fit model; note that the units of those coefficients are ‰$\Delta^{13}C$ per the units of each variable as given in Supporting Information Table S1. Sensitivity is an estimate of the largest potential effect of each variable on $\Delta^{13}C$ while holding all the other predictor variables constant and varying the variable of interest by its maximal range. This is equivalent to the slope of the line multiplied by the *x*-axis range within the panels of Supporting Information Figure S7. ΔBIC quantifies how much worse the model becomes when leaving that variable out of the model; larger values indicate more indispensable predictors.

TABLE 2 Bivariate correlation between leaf traits and $\Delta^{13}C$

Trait	Bivariate sample size	Bivariate correlation coefficient (*r*)	Residual variation explained (r^2)
Maximal photosynthetic rate per leaf area	393	−0.11	0.00
Maximal stomatal conductance	367	0.06	0.00
Specific leaf area	864	0.41	0.03
Nitrogen per leaf mass	1942	0.25	0.00
Leaf size	338	0.34	0.01
Nitrogen per leaf area	773	−0.47	0.11

Note. All traits were log_{10}-transformed before analysis. The correlation coefficient shows the simple bivariate comparison of the trait and $\Delta^{13}C$. Residual variation shows the r^2 for the relationship with the residuals from the selected climate–soils model (see Table 1).

There was a large collection of climate and soil variables that have small, but highly significant, effects (see geographic visualization of the model in Figure 3). It is also worth noting that they remain in the model despite our choice of the BIC approach, which is known for its strong preference for model parsimony (Burnham & Anderson, 2004; Kuha, 2004). The BIC-selected model variables include wind (more wind = less discrimination), growing season (longer growing season = greater discrimination) and silt (more silt in the soil = greater discrimination; see Supporting Information Figure S7).

3.2 | Plant trait-driven variation

With this dataset we can examine, on a global scale, whether the balance of supply and demand for CO_2 inside leaves, as captured by carbon isotopes, is correlated with maximal photosynthetic rates measured in optimal conditions. We find that area-based instantaneous measures of maximal photosynthesis are largely decoupled from carbon isotope discrimination ($r = -0.11$; Table 2; Supporting Information Figure S9). This implies that maximal flux rate is only weakly related to a time-integrative measure of p_c/p_a.

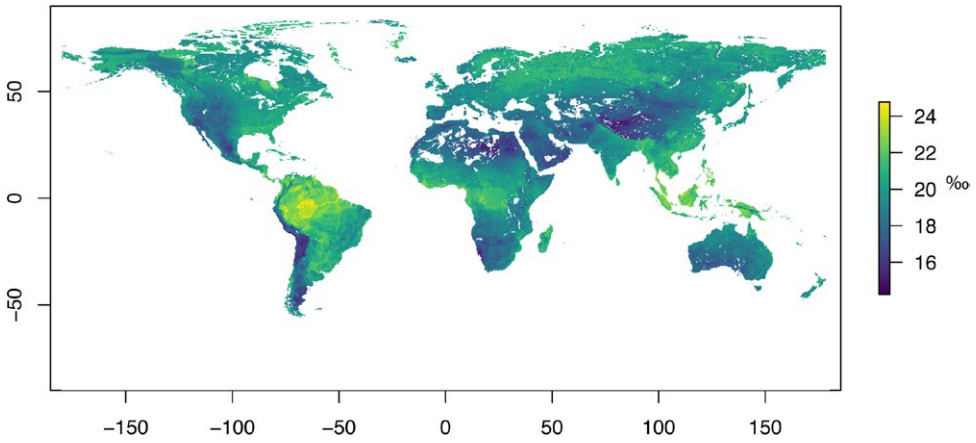

FIGURE 3 Predicted $\Delta^{13}C$ for C_3 photosynthesis across the globe, based on the model in Table 1. White indicates no data. In the case of land areas, the white parts are areas without sufficient soil data because they are aquatic or covered in glacial ice or because available data are not sufficient for them to be included in the Harmonized World Soil Database gridded soil data (see FAO, 2012) [Colour figure can be viewed at wileyonlinelibrary.com]

Two of the traits best correlated with discrimination were N per leaf area (N_{area}) and leaf size (Table 2 and Figure 4; specific leaf area was also correlated, probably in part owing to its link with N_{area}). Note that in this dataset there is only a weak correlation between N_{area} and measures of maximal photosynthetic rate: r = 0.22. This relationship is much weaker than is typically observed within a given climate zone (e.g., r = 0.61 from one Californian site; see Ackerly, 2004). The weakness of the relationship is probably attributable, at least in part, to the inclusion of species from both very dry and very wet climates (see discussion by Wright, Reich, & Westoby, 2003).

These relationships are linked to the effects of climate and soils on discrimination; for example, the correlation between discrimination and leaf size all but disappears after first accounting for climate and soils (Figure 4). In contrast, the relationship with N_{area} does not; it explains 11% of the remaining global variation even after accounting for climate and soils (Figure 4). On average, species with higher N_{area} showed lower discrimination (were operating at a lower p_c/p_a). Note that there is significant variation in N_{area} among species within sites; therefore, local variation driven by N_{area} independent of climate and soils is not accounted for in Figure 2 or 3.

3.3 | A living database of leaf $\Delta^{13}C$

Given that the links between the water and carbon cycles are likely to continue to be an area of active research, we have set up this database as a "living" database. The static version, on which this analysis is based, is available via zenodo (https://doi.org/10.5281/zenodo.569501). A dynamic, semantically versioned dataset will be distributed as an R package and updated via github releases (https://github.com/wcornwell/leaf13C). In this way, new data can be added, climate data can be updated to newly developed interpolated grids, and modeling efforts built on these data can use the most up-to-date dataset rather than a static one.

4 | DISCUSSION

Global fractionation of ^{13}C during photosynthesis, $\Delta^{13}C$, gives us a uniquely integrative view into p_c/p_a and plant water and carbon relationships more broadly. Our leaf-level understanding of controls on $\Delta^{13}C$, including controls on stomatal conductance, is detailed (Cernusak et al., 2013), but there are a number of complications involved in scaling up. We show that there is not a simple mapping of $\Delta^{13}C$ to one or a few macroclimatic variables, such as annual precipitation. Instead, numerous aspects of climate and soils affect the supply of water to the plant, the strength of the demand for water from the atmosphere, and the balance of CO_2 supply through the stomata and CO_2 demand at the sites of photosynthesis within the leaf.

In many cases, the statistical model presented here finds similar relationships compared with more local research and more detailed theory (see coefficients within Table 1). For example, we find a global-scale negative relationship between wind and $\Delta^{13}C$ that is similar to what would be expected based on theory (Grace, 1988). Likewise, the positive relationship we find with soil silt percentage is consistent with predictions from models of water dynamics across different soil textures (Tuzet, Perrier, & Leuning, 2003). For soil pH, our global-scale results are similar to those observed more locally (Viet et al., 2013; Weitner et al., 2007), although the underlying mechanism in both the global and local cases is unknown. Overall, the size of our dataset reveals that each individual relationship with $\Delta^{13}C$ has a relatively modest effect globally (see coefficients within Table 1), but there is nonetheless a very tight association between $\Delta^{13}C$ and a combination of soil and climate variables.

The environment–carbon isotope association ($r^2_{adj} = 0.60$) is much stronger than that for other functional aspects for leaves (and it would be stronger still when considering some plant functional types separately; see Supporting Information Figures S4 and S5 and Adams, Turnbull, Sprent, & Buchmann, 2016). The same model selection approach but with other leaf traits as the independent variable leads to a model with $r^2_{adj} = 0.28$ for leaf nitrogen per mass, $r^2_{adj} = 0.23$

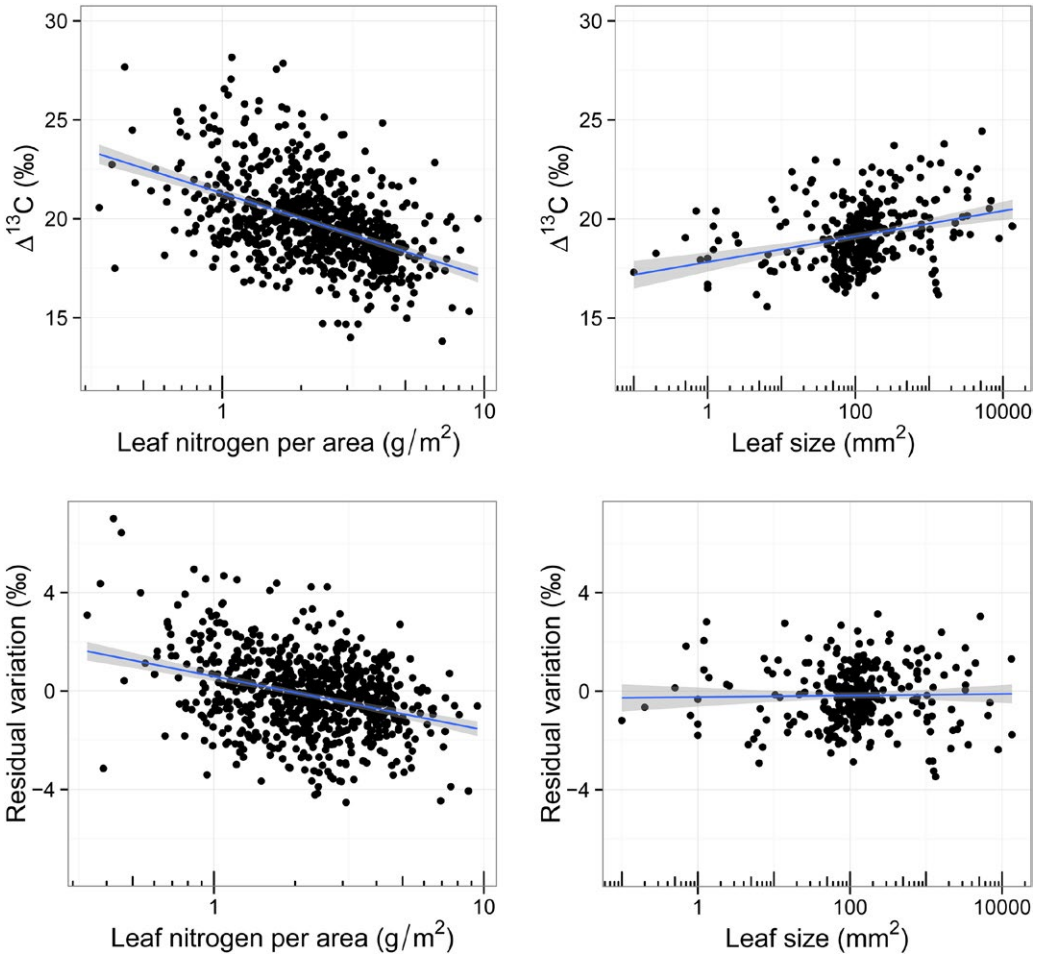

FIGURE 4 The relationship between two leaf traits (nitrogen per area and leaf size) and $\Delta^{13}C$. The raw bivariate relationships are shown in the top row. The relationship with the residuals from the climate–soil model (described in Table 1) are in the bottom row. Nitrogen per area has more explanatory power, in addition to climate and soils, compared with leaf size (see also Table 2) [Colour figure can be viewed at wileyonlinelibrary.com]

for specific leaf area, and $r^2_{adj} = 0.04$ for maximal rates of photosynthesis per leaf area (see also Wright et al., 2005). This implies that dynamic regulation of internal CO_2 is much more tightly linked to macroscale climate and soils than are leaf characteristics (on either mass or area bases), including the concentration of nitrogen and maximal photosynthetic rates, traits that often vary among species at very small scales (Ackerly, 2004).

The equation described by the BIC-selected model (Table 1) can be used as a predictive model together with global climate datasets to generate an expected discrimination via C_3 photosynthesis for every grid cell on the globe (Figure 3). Note that although this relationship describes a statistical expectation for each spot on the globe, there are still many sources of within-site variance in carbon isotope discrimination, both among and within species (Saugier, Ehleringer, Hall, & Farquhar, 1993); every leaf should not be expected to conform to this expectation, but the mean species value should be close to this value. Given the wealth of leaf-level physiological studies showing the effects of climate and soil on $\Delta^{13}C$, the fact that these results scale up to small but crucial global effects should not be surprising; however, it is contrary to analyses of smaller datasets (Diefendorf et al., 2010; Kohn, 2010); the authors of both these studies argued for a relatively simple precipitation–$\Delta^{13}C$ relationship.

4.1 | The balance of water supply and demand

Plant water relationships and carbon isotopic signals are considerably more complicated than solely mean annual precipitation. Macroclimatic variables in the final model included those that affect both the supply of water (including seasonality) and many variables that affect the atmospheric demand for water, including wind, atmospheric pressure and PET. These effects are not large individually; sensitivities varied from 0.6 to 6.0‰ (Table 1), but cumulatively they are crucial. Measuring and modeling atmospheric demand for water with respect to both time and space will be one of the crucial on-going challenges in understanding the water cycle at the global scale, and we expect that future work will both further constrain this relationship and more clearly tie this relationship to theory.

Three temperature-related variables were in the best BIC-selected model: PET, diurnal temperature range and frost frequency (Table 1). The role of temperature and its relationship with global maps

of PET are complex; it both influences water demand via effects on leaf temperature and vapor pressure deficit and it affects RuBisCO kinetics (Badger & Collatz, 1977; Bernacchi, Singsaas, Pimentel, Portis, & Long, 2001). Global estimates of PET are strongly correlated with mean annual temperature (see Supporting Information Figure S8). The PET could have both positive (via temperature-related mechanisms) and negative (via atmospheric demand) effects on $\Delta^{13}C$. In the selected model, aspects of atmospheric demand are accounted for by other variables (e.g., wind), and the positive (presumably temperature-related) effect remains in the model (Table 1 and Figure 2). The other two variables, diurnal temperature range and frost frequency, capture aspects of the daily temperature fluctuation, which differs greatly among environments across the globe, pointing to an important role for within-day temperature variation affecting the proportion of photosynthesis that occurs during optimal and suboptimal conditions. The omission of vapor pressure deficit from the best selected model might be attributable to current limitations in available maps. Daily temperature and humidity variation has important implications for the effective vapor pressure deficit during photosynthesis, one of many important effects that are not completely captured in currently available global maps. More precise maps of vapor pressure deficit would be very useful, and there has been recent progress on new methods for generating vapor pressure deficit maps (Zhang, Wu, Yan, Zhu, & Feng, 2014) from remote sensing products. The next generation of maps is likely to be much improved, and this question should be revisited at that point.

4.2 | Effects of atmospheric pressure

As has been shown in targeted studies (Körner, Farquhar, & Roksandic, 1988; Körner, Farquhar, & Wong, 1991; Zhu, Siegwolf, Durka, & Körner, 2010), discrimination is lower at high-elevation, low-atmospheric pressure sites, provided there are no elevational moisture gradients (Figure 2). What this large dataset reveals is that at the global scale the relationship with pressure and discrimination is triangular. At low elevation (= high atmospheric pressure), discrimination can be either high or low. At high elevation (= low atmospheric pressure), individuals that show high discrimination are absent (Figure 2). (This relationship becomes more linear when considering the partial residuals.) Considering only the effects of pressure, holding all else constant, there are at least two possible mechanisms. The first potential mechanism is the effect on water vapor concentrations. At low atmospheric pressure, the partial pressure of water in the atmosphere is lower, but the saturated partial pressure within the leaves maintains the same relationship with leaf temperature. This creates a larger leaf-to-air gradient in water vapor, increasing the atmospheric demand for water at high-elevation sites. Potentially, this may, through time, lead to greater water loss, which then might prompt stomatal regulation that reduces p_c/p_a and $\Delta^{13}C$ (see similar arguments by Körner et al., 1988; Körner et al., 1991; Wang et al., 2017). The second potential mechanism is the effect of a lower partial pressure of oxygen at high elevation, effectively increasing the affinity of RuBisCO for carbon dioxide, reducing p_c/p_a at a given stomatal conductance and reducing $\Delta^{13}C$. In addition to these two direct mechanisms, there are also indirect effects of elevation on plant traits that then influence fractionation (Körner et al., 1988).

4.3 | Soil

Fractionation is greatest (photosynthesis operates at the highest p_c/p_a) on silt soils (Table 1); that is, plants on silt soils have less restricted photosynthesis compared with sand and clay soils, which is consistent with the idea that silt soils have moisture-release curves that favor water-holding capacity and plant uptake in many conditions (Hillel, 1980).

The global pattern with less discrimination on high-pH soils (pH > 7) is striking (Figure 2) and consistent with local comparisons (Viet et al., 2013; Weitner et al., 2007), but the mechanism underlying this pattern has not been uncovered by previous detailed work. Part of the high bivariate r^2 (Figure 2) is undoubtedly the negative relationship between annual precipitation and soil pH, with lower pH more often found at sites with high rainfall. However, even after accounting for macroclimatic and other soil variables there is still a very large decline in model explanatory power when leaving pH out (ΔBIC =95.4; Table 1). Part of that might be related to N_{area}, which is slightly but significantly higher on high-pH soils (r^2 = 0.08, $p < 10^{-15}$, n = 1,014). Viewed within the framework of "least-cost" co-optimization theory for photosynthesis (Prentice, Dong, Gleason, Maire, & Wright, 2014; Wright et al., 2003), the observation that plants operate at lower p_c/p_a on higher pH soils suggests that in these situations plants are operating as if water is relatively expensive to acquire or, equivalently, as if soil nutrients are relatively cheap to acquire. Indeed, all else being equal, at higher pH one would generally expect a range of macro- and micronutrients, especially N, to be relatively more available (Marschner, 2012), which should decrease the per unit cost of their acquisition.

This could be an effect of soil development on both soil pH and macronutrient availability (especially P; see Porder, Vitousek, Chadwick, Chamberlain, & Hilley, 2007), which in turn affects overall site fertility and water relationships (Maire et al., 2015). It is also possible that the particular parent materials that weather to produce high-pH soils also weather to produce soils that have relatively high water-holding capacity.

4.4 | Growing season parameters and the challenge of understanding p_c/p_a across time-scales

Given that both environmental and stomatal aperture may change at very fast time-scales, understanding $\Delta^{13}C$ and p_c/p_a with respect to climate predictors on different time-scales is a difficult problem. We found explanatory power in climate variation at three scales: Daily, seasonal (i.e., during the growing season) and annual.

We expected climate parameters during the growing season (e.g., growing season temperature) to have especially strong explanatory power, but they did not. Instead, growing season length and the presence of a non-growing season added explanatory power to the model (Table 1). This could be the result of the physiologies of different species that are tuned to operate at high p_c/p_a at different

temperatures across the world. For example, a tundra sedge may operate at high p_c/p_a within a very different temperature range compared with a tropical forest tree. However, seasonal shifts to dry or cold conditions may affect p_c/p_a in both tropical and polar regions. During a shift to unfavorable conditions, more photosynthesis may occur at low p_c/p_a, perhaps because of the existence of transition periods, daily and/or seasonally, with conditions that allow photosynthesis but are not sufficiently favorable to permit high p_c/p_a.

4.5 | Plant traits

We suggest here a key association between N_{area} and $\Delta^{13}C$ both within and among sites (Figure 4). Comparing leaves of high with low N_{area}, the additional N_{area} is often in the form of a higher concentration of RuBisCO, which will lead to a lower internal CO_2 concentration and thus lower $\Delta^{13}C$, assuming that all else, including stomatal conductance, is held equal (Adams et al., 2016). The N_{area} is generally higher in areas of low precipitation (Wright et al., 2005). Essentially, as water supply drops and atmospheric water demand rises in arid environments, plants adjust both stomatal regulation and their ability to draw down p_c at a given conductance (Farquhar, Buckley, & Miller, 2002; Givnish, Wong, Stuart-Williams, Holloway-Phillips, & Farquhar, 2014; Prentice et al., 2011; Wright et al., 2003). There is also likely to be an important role for mesophyll conductance and how that varies with environmental gradients (Barbour et al., 2010; Evans & von Caemmerer, 2013; Vitousek et al., 1990), although at the global scale the data to constrain the importance of mesophyll conductance are not yet available.

4.6 | Conclusion

The global pattern in carbon isotope discrimination is very different from previously reported climate–trait relationships (Wright et al., 2005, 2004); we show that most of the variation in p_c/p_a is strongly associated with variation in climate and soils. Compared with other leaf traits, this functional convergence within climate zones is remarkable. In other words, when compared with global variation, in a given climate, species often have relatively different leaf morphologies and chemistries, but relatively similar CO_2 concentration at the site of carboxylation and thus $\Delta^{13}C$.

Leaf carbon isotopes provide a unique view into global photosynthesis. Our data-driven model predicts lowest fractionation (i.e., low $\Delta^{13}C$) in the major deserts of the world, the Tibetan Plateau and dry parts of the Andes. In contrast, the greatest fractionation is in the wet tropical forests of South America (especially close to the Amazon), Africa and Asia along with the silt soils on river flood plains of the far northern hemisphere (Figure 3). This is important empirical evidence about spatial variation in the way the water and carbon cycles are coupled across the globe.

Compared with datasets of instantaneous flux rates, $\Delta^{13}C$ data provide a uniquely time-integrated view into the carbon cycle, especially reflecting stomatal regulation of photosynthesis over a long time-frame. Building on this time-integrated feature, there have been efforts to scale up leaf- or stand-level models of $\Delta^{13}C$ to the globe (Ballantyne, Miller, Baker, Tans, & White, 2011; Lloyd & Farquhar, 1994; Prentice et al., 2014; Suits et al., 2005; Wang et al., 2017). This is a very useful model–data synthesis, and we hope that the model selection approach taken in this paper will be compared with more theory-driven mechanistic models to push forward a spatial understanding of the coupling of water and carbon cycles.

ACKNOWLEDGMENTS

Financial support came from the Australian Research Council, via the ARC-NZ Research Network for Vegetation Function and from the Netherlands Organization for Scientific Research (NWO) through its Open Competition Program of the section Earth and Life Sciences (ALW) grant no. 820.01.016. Computation was made possible by the Katana High Performance Computing facility in the Faculty of Science at the University of New South Wales.

DATA ACCESSIBILITY

The carbon isotope dataset is available in a stable form at the following https://doi.org/10.5281/zenodo.569501. An R library for easy download and use and a dynamic, "living" version of this dataset, welcoming additions, may be found at: https://github.com/wcornwell/leaf13C.

REFERENCES

Ackerly, D. (2004). Functional strategies of chaparral shrubs in relation to seasonal water deficit and disturbance. *Ecological Monographs*, *74*, 25–44. https://doi.org/10.1890/03-4022

Adams, M. A., Turnbull, T. L., Sprent, J. I., & Buchmann, N. (2016). Legumes are different: Leaf nitrogen, photosynthesis, and water use efficiency. *Proceedings of the National Academy of Sciences USA*, *113*, 4098–4103. https://doi.org/10.1073/pnas.1523936113

Badger, M. R., & Collatz, G. J. (1977). Studies on the kinetic mechanism of ribulose-1,5-bisphosphate carboxylase and oxygenase reactions, with particular reference to the effect of temperature on kinetic parameters. *Carnegie Institution of Washington Year Book*, *76*, 355–361.

Ballantyne, A., Miller, J., Baker, I., Tans, P., & White, J. (2011). Novel applications of carbon isotopes in atmospheric CO_2: What can atmospheric measurements teach us about processes in the biosphere? *Biogeosciences*, *8*, 3093–3106.

Barbour, M. M., Warren, C. R., Farquhar, G. D., Forrester, G., & Brown, H. (2010). Variability in mesophyll conductance between barley genotypes, and effects on transpiration efficiency and carbon isotope discrimination. *Plant, Cell and Environment*, *33*, 1176–1185. https://doi.org/10.1111/j.1365-3040.2010.02138.x

Bartoń, K. (2016). *MuMIn: Multi-model Inference* (R Package Version 1.15.6). https://CRAN.R-project.org/package=MuMIn

Batjes, N. (2012). *ISRIC-WISE derived soil properties on a 5 by 5 arc-minutes global grid (ver. 1.2)*. Wageningen, The Netherlands: ISRIC.

Beer, C., Ciais, P., Reichstein, M., Baldocchi, D., Law, B., Papale, D., … Frank, D. (2009). Temporal and among-site variability of inherent water use efficiency at the ecosystem level. *Global Biogeochemical Cycles*, *23*, GB2018. https://doi.org/10.1029/2008GB003233

Bernacchi, C., Singsaas, E., Pimentel, C., Portis, A. Jr, & Long, S. (2001). Improved temperature response functions for models of Rubisco-limited photosynthesis. *Plant, Cell and Environment*, *24*, 253–259. https://doi.org/10.1111/j.1365-3040.2001.00668.x

Bowling, D. R., Tans, P. P., & Monson, R. K. (2001). Partitioning net ecosystem carbon exchange with isotopic fluxes of CO_2. *Global Change Biology*, *7*, 127–145. https://doi.org/10.1046/j.1365-2486.2001.00400.x

Breheny, P., & Burchett, W. (2013). Visualization of Regression Models Using visreg. The R Journal, *9*, 56–71.

Brooks, J. R., Flanagan, L. B., Buchmann, N., & Ehleringer, J. R. (1997). Carbon isotope composition of boreal plants: Functional grouping of life forms. *Oecologia*, *110*, 301–311. https://doi.org/10.1007/s004420050163

Brüggemann, N., Gessler, A., Kayler, Z., Keel, S., Badeck, F., Barthel, M., … Bahn, M. (2011). Carbon allocation and carbon isotope fluxes in the plant soil-atmosphere continuum: A review. *Biogeosciences*, *8*, 3457–3489. https://doi.org/10.5194/bg-8-3457-2011

Buckley, T. N., & Mott, K. A. (2013). Modelling stomatal conductance in response to environmental factors. *Plant, Cell and Environment*, *36*, 1691–1699. https://doi.org/10.1111/pce.12140

Burnham, K. P., & Anderson, D. R. (2004). Multimodel inference: Understanding AIC and BIC in model selection. *Sociological Methods and Research*, *33*, 261–304. https://doi.org/10.1177/0049124104268644

Cernusak, L. A., Tcherkez, G., Keitel, C., Cornwell, W. K., Santiago, L. S., Knohl, A., … Wright, I. J. (2009). Why are non-photosynthetic tissues generally ^{13}C enriched compared with leaves in C_3 plants? Review and synthesis of current hypotheses. *Functional Plant Biology*, *36*, 199–213.

Cernusak, L. A., Ubierna, N., Winter, K., Holtum, J. A., Marshall, J. D., & Farquhar, G. D. (2013). Environmental and physiological determinants of carbon isotope discrimination in terrestrial plants. *New Phytologist*, *200*, 950–965. https://doi.org/10.1111/nph.12423

Chadwick, O. A., Derry, L., Vitousek, P. M., Huebert, B. J., & Hedin, L. O. (1999). Changing sources of nutrients during four million years of ecosystem development. *Nature*, *397*, 491–497. https://doi.org/10.1038/17276

Dawson, T. E., Mambelli, S., Plamboeck, A. H., Templer, P. H., & Tu, K. P. (2002). Stable isotopes in plant ecology. *Annual Review of Ecology and Systematics*, *33*, 507–559. https://doi.org/10.1146/annurev.ecolsys.33.020602.095451

Diefendorf, A. F., Mueller, K. E., Wing, S. L., Koch, P. L., & Freeman, K. H. (2010). Global patterns in leaf ^{13}C discrimination and implications for studies of past and future climate. *Proceedings of the National Academy of Sciences USA*, *107*, 5738–5743. https://doi.org/10.1073/pnas.0910513107

Ehleringer, J., Field, C., Lin, Z. F., & Kuo, C. Y. (1986). Leaf carbon isotope and mineral composition in subtropical plants along an irradiance cline. *Oecologia*, *70*, 520–526. https://doi.org/10.1007/BF00379898

Evans, J., Sharkey, T., Berry, J., & Farquhar, G. (1986). Carbon isotope discrimination measured concurrently with gas exchange to investigate CO_2 diffusion in leaves of higher plants. *Functional Plant Biology*, *13*, 281–292.

Evans, J. R., & von Caemmerer, S. (2013). Temperature response of carbon isotope discrimination and mesophyll conductance in tobacco. *Plant, Cell and Environment*, *36*, 745–756. https://doi.org/10.1111/j.1365-3040.2012.02591.x

FAO. (2012). *Harmonized World Soil Database (Version 1.2)*. http://www.fao.org/soils-portal/soil-survey/soil-maps-and-databases/harmonized-world-soil-database-v12/en/

Farquhar, G. D., Buckley, T. N., & Miller, J. M. (2002). Optimal stomatal control in relation to leaf area and nitrogen content. *Silva Fennica*, *36*, 625–637. https://doi.org/10.14214/sf.530

Farquhar, G. D., Ehleringer, J. R., & Hubick, K. T. (1989). Carbon isotope discrimination and photosynthesis. *Annual Review of Plant Biology*, *40*, 503–537. https://doi.org/10.1146/annurev.pp.40.060189.002443

Farquhar, G. D., O'Leary, M. H., & Berry, J. A. (1982). On the relationship between carbon isotope discrimination and the intercellular carbon dioxide concentration in leaves. *Functional Plant Biology*, *9*, 121–137. https://doi.org/10.1071/PP9820121

Farquhar, G. D., & Richards, R. (1984). Isotopic composition of plant carbon correlates with water-use efficiency of wheat genotypes. *Functional Plant Biology*, *11*, 539–552. https://doi.org/10.1071/PP9840539

Givnish, T. J., Wong, S. C., Stuart-Williams, H., Holloway-Phillips, M., & Farquhar, G. D. (2014). Determinants of maximum tree height in eucalyptus species along a rainfall gradient in Victoria, Australia. *Ecology*, *95*, 2991–3007.

Grace, J. (1988). Plant response to wind. *Agriculture, Ecosystems and Environment*, *22–23*, 71–88.

Graham, M. H. (2003). Confronting multicollinearity in ecological multiple regression. *Ecology*, *84*, 2809–2815. https://doi.org/10.1890/02-3114

Grueber, C., Nakagawa, S., Laws, R., & Jamieson, I. (2011). Multimodel inference in ecology and evolution: Challenges and solutions. *Journal of Evolutionary Biology*, *24*, 699–711. https://doi.org/10.1111/j.1420-9101.2010.02210.x

Hijmans, R. J. (2014). *Raster: Geographic data analysis and modeling (R package version 2.2-5)*. https://CRAN.R-project.org/package=raster

Hillel, D. (1980). *Fundamentals of soil physics*. London, UK: Academic Press.

Jones, H. G. (1992). *Plants and microclimate: A quantitative approach to environmental plant physiology*. Cambridge, UK: Cambridge University Press.

Jordan, D. N., & Smith, W. K. (1995). Radiation frost susceptibility and the association between sky exposure and leaf size. *Oecologia*, *103*, 43–48. https://doi.org/10.1007/BF00328423

Kaplan, J. O., Prentice, I. C., & Buchmann, N. (2002). The stable carbon isotope composition of the terrestrial biosphere: Modeling at scales from the leaf to the globe. *Global Biogeochemical Cycles*, *16*, 8-1–8-11. https://doi.org/10.1029/2001GB001403

Kikuzawa, K., Onoda, Y., Wright, I. J., & Reich, P. B. (2013). Mechanisms underlying global temperature-related patterns in leaf longevity. *Global Ecology and Biogeography*, *22*, 982–993. https://doi.org/10.1111/geb.12042

Kohn, M. J. (2010). Carbon isotope compositions of terrestrial C_3 plants as indicators of (paleo) ecology and (paleo) climate. *Proceedings of the National Academy of Sciences USA*, *107*, 19691–19695. https://doi.org/10.1073/pnas.1004933107

Körner, C., Farquhar, G., & Roksandic, Z. (1988). A global survey of carbon isotope discrimination in plants from high altitude. *Oecologia*, *74*, 623–632. https://doi.org/10.1007/BF00380063

Körner, C., Farquhar, G., & Wong, S. (1991). Carbon isotope discrimination by plants follows latitudinal and altitudinal trends. *Oecologia*, *88*, 30–40. https://doi.org/10.1007/BF00328400

Kuha, J. (2004). AIC and BIC comparisons of assumptions and performance. *Sociological Methods and Research*, *33*, 188–229. https://doi.org/10.1177/0049124103262065

Lloyd, J., & Farquhar, G. D. (1994). ^{13}C discrimination during CO_2 assimilation by the terrestrial biosphere. *Oecologia*, *99*, 201–215. https://doi.org/10.1007/BF00627732

Maire, V., Wright, I. J., Prentice, I. C., Batjes, N. H., Bhaskar, R., Bodegom, P. M., … Ordonez, A. (2015). Global effects of soil and climate on leaf photosynthetic traits and rates. *Global Ecology and Biogeography*, *24*, 706–717. https://doi.org/10.1111/geb.12296

Marschner, H. (2012). *Mineral nutrition of higher plants*. Stuttgart, Germany: Academic Press.

Monteith, J., & Unsworth, M. (2007). *Principles of environmental physics*. Academic Press.

New, M., Lister, D., Hulme, M., & Makin, I. (2002). A high-resolution data set of surface climate over global land areas. *Climate Research*, *21*, 1–25. https://doi.org/10.3354/cr021001

Nier, A. O., & Gulbransen, E. A. (1939). Variations in the relative abundance of the carbon isotopes. *Journal of the American Chemical Society*, *61*, 697–698. https://doi.org/10.1021/ja01872a047

Porder, S., Vitousek, P. M., Chadwick, O. A., Chamberlain, C. P., & Hilley, G. E. (2007). Uplift, erosion, and phosphorus limitation in terrestrial ecosystems. *Ecosystems*, *10*, 159–171. https://doi.org/10.1007/s10021-006-9011-x

Prentice, I. C., Dong, N., Gleason, S. M., Maire, V., & Wright, I. J. (2014). Balancing the costs of carbon gain and water transport: Testing a new theoretical framework for plant functional ecology. *Ecology Letters*, *17*, 82–91. https://doi.org/10.1111/ele.12211

Prentice, I. C., Meng, T., Wang, H., Harrison, S. P., Ni, J., & Wang, G. (2011). Evidence of a universal scaling relationship for leaf CO_2 drawdown along an aridity gradient. *New Phytologist*, *190*, 169–180. https://doi.org/10.1111/j.1469-8137.2010.03579.x

R Core Team. (2013). *R: A language and environment for statistical computing*. Vienna, Austria: R Foundation for Statistical Computing.

Saugier, B., Ehleringer, J. R., Hall, A. E., & Farquhar, G. D. (1993). *Stable isotopes and plant carbon-water relations*. Amsterdam, The Netherlands: Elsevier.

Schulze, E. D., Williams, R., Farquhar, G., Schulze, W., Langridge, J., Miller, J., & Walker, B. H. (1998). Carbon and nitrogen isotope discrimination and nitrogen nutrition of trees along a rainfall gradient in Northern Australia. *Functional Plant Biology*, *25*, 413–425. https://doi.org/10.1071/PP97113

Stewart, G. R., Turnbull, M., Schmidt, S., & Erskine, P. (1995). ^{13}C natural abundance in plant communities along a rainfall gradient: A biological integrator of water availability. *Functional Plant Biology*, *22*, 51–55.

Still, C. J., Berry, J. A., Collatz, G. J., & DeFries, R. S. (2003). Global distribution of c3 and c4 vegetation: Carbon cycle implications. *Global Biogeochemical Cycles*, *17*, 6-1–6-14.

Suits, N. S., Denning, A. S., Berry, J., Still, C., Kaduk, J., Miller, J., & Baker, I. (2005). Simulation of carbon isotope discrimination of the terrestrial biosphere. *Global Biogeochemical Cycles*, *19*, GB1017. https://doi.org/10.1029/2003GB002141

Tuzet, A., Perrier, A., & Leuning, R. (2003). A coupled model of stomatal conductance, photosynthesis and transpiration. *Plant, Cell and Environment*, *26*, 1097–1116. https://doi.org/10.1046/j.1365-3040.2003.01035.x

Venables, W. N., & Ripley, B. D. (2002). *Modern applied statistics with S*. New York, NY: Springer.

Viet, H. D., Kwak, J.-H., Lee, K.-S., Lim, S.-S., Matsushima, M., Chang, S., … Choi, W.-J. (2013). Foliar chemistry and tree ring $\delta^{13}C$ of *Pinus densiflora* in relation to tree growth along a soil pH gradient. *Plant and Soil*, *363*, 101–112. https://doi.org/10.1007/s11104-012-1301-9

Virgona, J., & Farquhar, D. (1996). Genotypic variation in relative growth rate and carbon isotope discrimination in sunflower is related to photosynthetic capacity. *Functional Plant Biology*, *23*, 227–236. https://doi.org/10.1071/PP9960227

Vitousek, P. M., Field, C. B., & Matson, P. A. (1990). Variation in foliar $\delta^{13}C$ in Hawaiian *Metrosideros polymorpha*: A case of internal resistance? *Oecologia*, *84*, 362–370. https://doi.org/10.1007/BF00329760

Vogel, S. (1970). Convective cooling at low airspeeds and the shapes of broad leaves. *Journal of Experimental Botany*, *21*, 91–101. https://doi.org/10.1093/jxb/21.1.91

Wang, H., Prentice, I. C., Keenan, T. F., Davis, T. W., Wright, I. J., Cornwell, W. K., … Peng, C. (2017). Towards a universal model for carbon dioxide uptake by plants. *Nature Plants*, *3*, 734. https://doi.org/10.1038/s41477-017-0006-8

Weitner, A., Dupouey, J., Lefèvre, Y., Bréda, N., Badeau, V., Ferhi, A., … Thimonier, A. (2007). Roles of soil chemistry and water availability in site-related $\delta^{13}C$ variations in French beech forests. *Tree Physiology*, *27*, 1043–1051.

Whittaker, R. H. (1975). *Communities and ecosystems*. New York, NY: Macmillan Publishing.

Wolf, S., Eugster, W., Ammann, C., Häni, M., Zielis, S., Hiller, R., … Buchmann, N. (2013). Contrasting response of grassland versus forest carbon and water fluxes to spring drought in switzerland. *Environmental Research Letters*, *8*, 035007. https://doi.org/10.1088/1748-9326/8/3/035007

Wright, I. J., Reich, P. B., Cornelissen, J. H., Falster, D. S., Groom, P. K., Hikosaka,K.,…Westoby,M.(2005).Modulationofleafeconomictraits and trait relationships by climate. *Global Ecology and Biogeography*, *14*, 411–421. https://doi.org/10.1111/j.1466-822x.2005.00172.x

Wright, I. J., Reich, P. B., & Westoby, M. (2003). Least-cost input mixtures of water and nitrogen for photosynthesis. *The American Naturalist*, *161*, 98–111.

Wright, I. J., Reich, P. B., Westoby, M., Ackerly, D. D., Baruch, Z., Bongers, F., … Villar, R. (2004). The worldwide leaf economics spectrum. *Nature*, *428*, 821–827. https://doi.org/10.1038/nature02403

Zhang, H., Wu, B., Yan, N., Zhu, W., & Feng, X. (2014). An improved satellite-based approach for estimating vapor pressure deficit from MODIS data. *Journal of Geophysical Research: Atmospheres*, *119*, 12256–12271.

Zhu, Y., Siegwolf, R. T., Durka, W., & Körner, C. (2010). Phylogenetically balanced evidence for structural and carbon isotope responses in plants along elevational gradients. *Oecologia*, *162*, 853–863. https://doi.org/10.1007/s00442-009-1515-6

Zomer, R. J., Trabucco, A., Bossio, D. A., & Verchot, L. V. (2008). Climate change mitigation: A spatial analysis of global land suitability for clean development mechanism afforestation and reforestation. *Agriculture, Ecosystems and Environment*, *126*, 67–80. https://doi.org/10.1016/j.agee.2008.01.014

BIOSKETCH

This research team grew from an ARC-NZ Research Network for Vegetation Function meeting that assembled an early version of this dataset, including data from published and unpublished datasets on leaves collected from across the world. The team includes many of the original data collectors and those who assembled, curated and analyzed the data. Within the team there is a mix of plant physiologists, familiar with the mechanisms affecting carbon isotopes in plants, and ecologists interested in patterns and processes at larger scales.

SUPPORTING INFORMATION

Additional Supporting Information may be found online in the supporting information tab for this article.

How to cite this article: Cornwell WK, Wright IJ, Turner J, et al. Climate and soils together regulate photosynthetic carbon isotope discrimination within C_3 plants worldwide. *Global Ecol Biogeogr*. 2018;27:1056–1067. https://doi.org/10.1111/geb.12764